Evaluation of CHF Correlation Model Performance in MATRA for Various Rod Bundle Geometries

Seojun Park, Kyung Mo Kim*
Department of Energy Engineering, Korea Institute of Energy Technology (KENTECH), Kentech-gil 21, Naju-si, Jeollanam-do 58330, Republic of Korea
seojun@kentech.ac.kr, kmokim@kentech.ac.kr

***Keywords : Critical Heat Flux, MATRA, Model/Correlation, Two-phase Flow, Boiling**

1. Introduction

The occurrence of critical heat flux (CHF) is an important phenomenon in thermal-hydraulic design of light water reactors, because it results in considerable reduction in heat transfer between fuel rods and coolant. To ensure reactor safety, accurate CHF prediction is essential; consequently, various correlations and prediction models have been developed. These CHF prediction methodologies have been implemented into subchannel analysis codes such as MATRA (Multichannel Analyzer for steady-states and Transients in Rod Arrays), to predict CHF within fuel assembly geometries under off-normal conditions, including Design Basis Accidents (DBAs) [1].

However, CHF in a fuel assembly is governed by multiple variables, such as coupling effects between local parameters in individual subchannels, the geometric configuration, and the radial and axial power distribution of fuels. Therefore, whenever a fuel design is modified, CHF experiments have been conducted to develop specific correlations; the applicability of existing correlations and prediction models may be limited to specific configurations. To overcome these limitations, a new methodology is required that can accurately predict CHF across various fuel assembly designs and thermal-hydraulic conditions.

To develop an enhanced CHF prediction model, pre-existing CHF correlations and prediction models must be closely analyzed according to fuel assembly designs and the thermal-hydraulic conditions and be evaluated to identify the factors limiting their performance. In this study, predictive capability of the existing CHF correlations on several fuel assembly designs was evaluated with analysis on underlying causes of deviations between experimental data and predictions, thereby deriving key elements for improving performance.

2. Methods

2.1. Reference CHF data

To evaluate the CHF prediction capability in a fuel assembly design of the MATRA with three different correlations, CHF database collected by EPRI [2] is employed in this study. A total 100 experimental conditions with three fuel assembly geometries were analyzed by MATRA. The fuel assembly designs are classified as 5×5 standard array, a 5×5 cruciform array, and a 5×5 array with a big rod, as shown in Fig. 1.

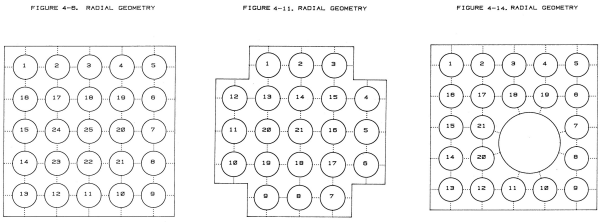

Fig 1. Geometries of rod configuration

The experimental conditions for the selected data are summarized in Table I.

Table I. Inlet conditions of selected CHF database

Variables	Range
Inlet mass velocity	407 ~ 5112 (kg/m^2 · s)
Inlet temperature	450.0 ~ 610.9 (K)
Exit pressure	6.18 ~ 16.72 (MPa)
Rod diameter	9.5 ~ 11.2 (mm)
Rod length	1219 ~ 2438 (mm)
Rod to rod gap	12.6 ~ 14.73 (mm)
Axial geometry slice gap	30.05 ~ 30.48 (mm)
Axial power profile	Uniform

2.2. Analysis methodology

The identification of CHF by MATRA was performed by increasing the heat flux step by step with 100 kW/m^2 interval from 0% to 80% of the experimentally observed CHF value under corresponding inlet conditions. To accurately capture the CHF occurrence, increment of heat flux is adjusted as 10 kW/m^2 from 80% to 120% of experimentally determined CHF values.

Table II summarizes the correlation models employed during analyses for estimation of two-phase parameters in the individual subchannels.

Table II. Models employed to compute the parameters related to the two-phase flow

Thermal-hydraulic analysis	Correlation models
Subcooled void fraction	Homogeneous model
Bulk void fraction	Chexal-Lellouche model
Two-phase friction multiplier	Armand model
Type of void draft correction factor	KAERI (Independent of flow regime)

2.3. CHF correlation

In this study, three CHF correlations implemented in MATRA-X0; B&W-2, W-3, and WRB-1 correlations [3, 4, 5], were used for the comparative analysis of their predictive performance.

2.3.1. B&W-2 correlation

B&W-2 (Babcock and Wilcox, 1969) [3] correlation formula was developed and optimized specifically for 15×15 fuel rod bundle geometries and is recognized for its high predictive accuracy within the pressure range of 2000~2400 psia [3]. The formula expressed as follows (1):

$$Q_{CHF} = \frac{1.155 - 0.407(D_h)}{(12.71)(3.053 \times 10^6 G)^A} \times [(0.3702 \times 10^8) \times (0.59137 \times 10^{-6} G)^B - 0.15208 h_{fg} \cdot G], \quad (1)$$

$$A = 0.71186 + (2.0729 \times 10^{-4}) \cdot (P - 1000), \quad (2)$$

$$B = 0.834 + (6.8479 \times 10^{-4})(P - 2000), \quad (3)$$

where D_h is heated equivalent diameter (in), G is mass velocity $(lb/hr \cdot ft^2)$, and h_{fg} is heat of vaporization $(BTU/lb \cdot °R)$.

If axial power profile is non-uniform, F_{APk} (axial power factor at node k) is divided on formula (1). F_{APk} is defined as follows (4):

$$F_{APk} = 1 + \frac{Y-1}{1-\bar{G}}, \quad (4)$$

$$Y = \frac{\sum_{j=2}^{k} q_j (z_{j+1} - z_j)}{q_j z_j}, \quad (5)$$

where $\bar{G}$ is memory effect controlled suggested by Tong [4]. $\bar{G}$ contribute the impact of upstream heat input to downstream DNB occurrence. It is defined as follows:

$$\bar{G} \approx \frac{1 - e^{-CL}}{CL}, \quad (6)$$

$$C = \frac{0.15(1-x)^{4.31}}{(10^{-6}G)^{0.478}}, \quad (7)$$

where C is energy dissipation rate (in^{-1}) suggested by Tong, and L is heated length (in).

2.3.2. W-3 correlation

W-3 (Westinghouse, 1967) correlation formula is expressed as follows [4]:

$$Q_{CHF,simple\ tube} = 10^6 \times \left\{ \begin{array}{c} [2.002 - 0.4302(0.001p)] \\ +[0.1722 - 0.0984(0.001p)] \\ \times e^{[18.77x - 0.004129p \cdot x]} \\ \times [(0.1484 - 1.596x + 0.1729x|x|)(10^{-6}G) + 1.037] \\ \times (1.157 - 0.869x) \\ \times [0.2664 + 0.8357e^{-3.151 D_h}] \\ \times [0.8258 + 0.000794(H_{sat} - H_{in})] \end{array} \right\} \quad (8)$$

where x is local quality, H_{sat} is saturated liquid enthalpy (Btu/lb), and H_{in} is inlet coolant enthalpy (Btu/lb).

W-3 correlation is developed with simple tube, with applications of correction factors, i.e., F_{CW} (cold-wall factor), F_S (simple grid factor) and $F_{GRID(RL)}$ (mixing vane grid factor). To consider the effects of axial power profile, F_{APk} is divided on the correlation. Revised W-3 correlation is expressed as follows (9):

$$Q_{CHF} = Q_{CHF,simple\ tube} \times \frac{F_{CW} F_{GRID}}{F_{APk}}, \quad (9)$$

$$F_{CW} = \left\{ \begin{array}{c} 1 - \left(1 - \frac{D_{hy}}{D_h}\right) \\ \times \left[\begin{array}{c} 13.76 - 1.372e^{1.78x} - 4.732(10^{-6}G)^{-0.0535} \\ -0.0619\left(\frac{p}{1000}\right)^{0.14} - 8.509 D_h^{0.107} \end{array} \right] \end{array} \right\},$$

$$F_{GRID(S)} = 1.0 + 0.03 \times 10^{-6} G \left(\frac{TDC}{0.019}\right)^{0.35},$$

$$F_{GRID(RL)} = F_g \times \left\{ \begin{array}{c} (1.445 - 0.0371L)\left(\frac{p}{225.896}\right)^{0.5} \left[e^{(x+0.2)^2} - 0.73\right] \\ +K_S \times 10^{-6} G \left(\frac{TDC}{0.019}\right)^{0.035} \end{array} \right\},$$

where D_{hy} is wetted equivalent diameter, TDC is turbulent crossflow mixing parameter, F_g and K_s are each grid factor and grid shape constant.

2.3.3 WRB-1 correlation model

WRB-1 (Westinghouse, 1976) correlation is a model that incorporates the effects of mixing vane grids. Since the grid effects are already integrated into the correlation, no additional factor corrections are required. Its formula is expressed as follows [5]:

(1) $Q_{CHF} = A - B \cdot x_{loc}$,
(2) $A = A[P, G_{loc}, L, G_{sp}, D_g]$,
(3) $B = B[P, G_{loc}, L]$,
(4) $Q_{chf} = PF + A_1 + B_3 \cdot G_{loc} - B_4 \cdot x_{loc} \cdot G_{loc}$,

where x_{loc} is local thermodynamic quality, G_{sp} is mixing vane grid spacing (in), D_g is distance to grid (in), and PF is performance factor.

3. Results & Discussion

The predictive capability of the CHF correlations according to the fuel assembly designs are compared as shown in Figure 2, with a metric of prediction to measurement ratio (P/M). Details of quantitative metrics are also presented in Table III. As shown in Fig 2, W-3 correlation exhibited the lowest standard deviation of P/M with mean P/M of 1.015, indicating the best agreement with the experimental data.

In contrast, B&W-2 and WRB-1 correlations showed comparably poor prediction accuracy than W-3 correlation. Not only B&W-2 model and WRB-1 model showed higher standard deviation, but also B&W-2 model demonstrated mean P/M of 0.576, which deviates significantly from the reference value 1.0.

As shown in 2(a), 2(b), 2(c), underprediction of B&W-2 correlation and overprediction of WRB-1 correlation observed consistently despite different fuel assembly designs, except that the WRB-1 correlation showed relatively good agreement with the experimental data for a cruciform fuel assembly. The observed conservative

prediction of the B&W-2 correlation is consistent with previous studies [3, 4]. In addition, the superior performance of the W-3 correlation compared to the WRB-1 correlation was also reported by Anderson and Wolfhope's work [5].

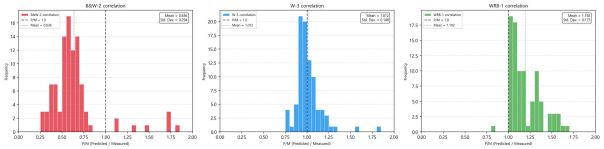

(a) 5x5 standard array

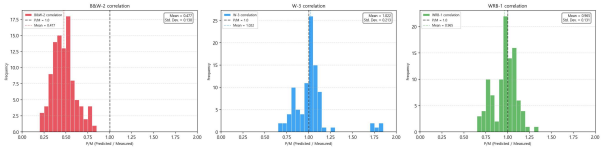

(b) 5x5 cruciform array

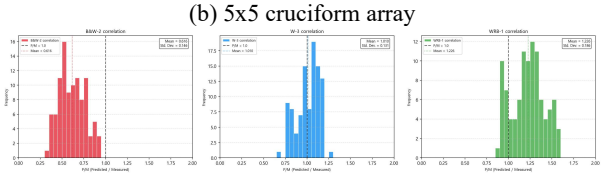

(c) 5x5 array with big rod

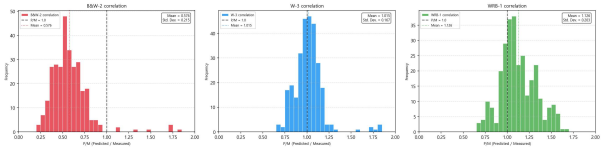

(d) Entire array

Fig 2. Prediction data histogram according to fuel rod assembly geometries

Table III. P/M ratio metrics for each fuel rod assembly

Geometry	Model	Mean	Std. Dev.
(a) 5x5 standard	B&W-2	0.636	0.294
	W-3	1.012	0.148
	WRB-1	1.192	0.175
(b) 5x5 cruciform	B&W-2	0.477	0.130
	W-3	1.022	0.213
	WRB-1	0.965	0.131
(c) 5x5 with big rod	B&W-2	0.616	0.146
	W-3	1.010	0.131
	WRB-1	1.226	0.186
(d) Entire	B&W-2	0.576	0.215
	W-3	1.015	0.167
	WRB-1	1.126	0.203

The location of CHF occurrence could be also identified during the analysis. Because CHF in a fuel assembly occurs at specific fuel rods and axial locations due to local thermal-hydraulic conditions and the design criteria are determined by the minimum thermal margin (MDNBR) of the entire assembly, accurately predicting the location of CHF occurrence is essential to correctly evaluate the validity of the actual limit thermal margin and mixing/flow distribution analysis and to prevent over- or under-estimation of safety margin.

Figure 3 illustrates the axial positions at which CHF occur, as well as the specific locations on the fuel rod where CHF is predicted by the CHF correlations. The colored *xy*-planes represent the lowest axial elevation among all CHF locations predicted by the models. The colored number circles indicate the minimum predicted CHF location on each rod, and the black cylinders represent the CHF rod from EPRI experiment. As shown in Fig. 3, it was observed that WRB-1 correlation failed to identify the fuel rod at which the CHF actually occurs. Although B&W-2 and W-3 correlations identified the fuel rod where the CHF occurs, they predicted multiple occurrences of the CHF. Predicting that CHF occurs in a greater number of fuel rods than actually observed is a conservative result that underestimates the thermal margin. However, this also indicates that the local thermal-hydraulic parameters, as well as mixing and grid effects, are simulated inaccurately, which is undesirable with respect to the physical validity of the analysis model and the optimization of the design.

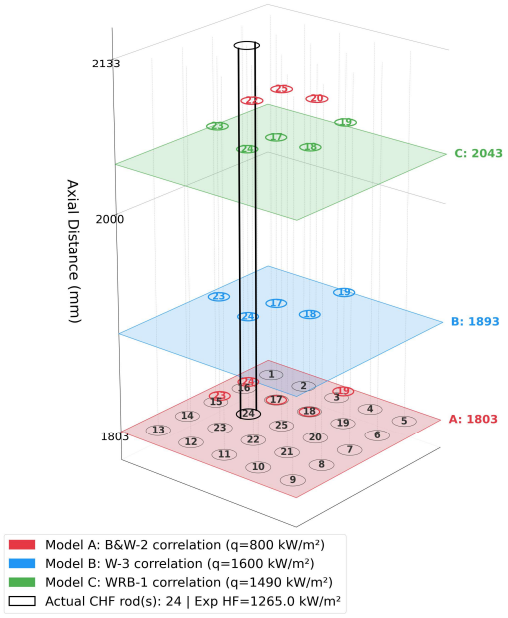

Fig 3. Specific data of CHF location prediction result and comparison with experiment data at 5×5 standard array (P = 12.41 MPa, T = 566.5 K, G= 2703 kg/m^2 · s)

Figure 4 illustrates the equilibrium quality, mass flux, enthalpy, density at the height where the thermocouples are located for the corresponding condition of Figure 3. Specifically, Fig. 4(a) displays the distributions of thermal-hydraulic parameters, while Fig. 4(b) shows the *z*-score of predictions for the individual parameters. And Fig. 4(c) displays the average z-score of 2×2 subchannel regions surrounding each rod. Extreme deviations were observed near the rod where the actual CHF occurred, with z-scores of +1.51 for equilibrium quality, +1.51 for enthalpy, and -1.46 for mixture density. In contrast, the mass flux exhibited a relatively smaller deviation.

Figure 5 compares the z-score of thermal-hydraulic parameters between CHF rods and non-CHF rods for the investigated rod bundles. The influence of each parameter was evaluated by calculating z-scores based

on the average values of the four subchannels surrounding each rod and comparing the results between the two rod categories. The mass flux displayed relatively minor deviations between CHF and non-CHF rods across all three configurations, indicating that the effect of mass flux on the CHF is insignificant. In contrast, equilibrium quality, enthalpy, and density show significant differences. Considering that W-3 model accurately predicted CHF locations compared to the others in Fig. 2(d), these differences stem from CHF correlations themselves rather than the two-phase flow models. Notably, the 5×5 cruciform configuration exhibited a significant variation in quality relative to other configurations. Given that the WRB-1 model demonstrated substantial improvement for this particular shape, it can be inferred that the WRB-1 model considers a considerable influence of quality within the correlation. Conversely, since the B&W-2 correlation did not display a marked change or improvement for the 5×5 cruciform array, it suggests that the impact of quality in this context is minimal.

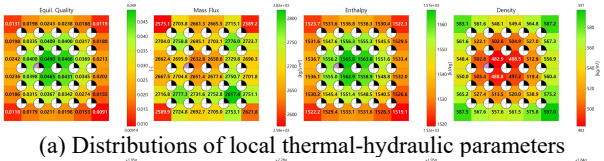

(a) Distributions of local thermal-hydraulic parameters

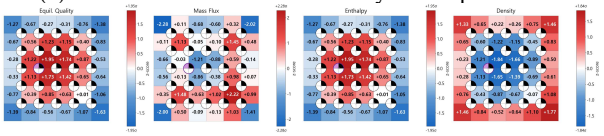

(b) z-score of thermal-hydraulic parameters

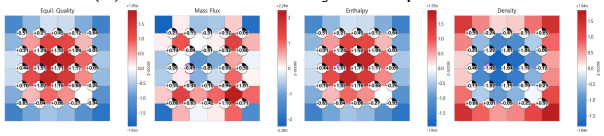

(c) average z-score of 2x2 subchannel regions surrounding each rod

Fig 4. Specific data of thermal-hydraulic parameters prediction results on at 5×5 standard array (P = 12.41MPa, T = 566.5 K, G= 2703 kg/m² · s)

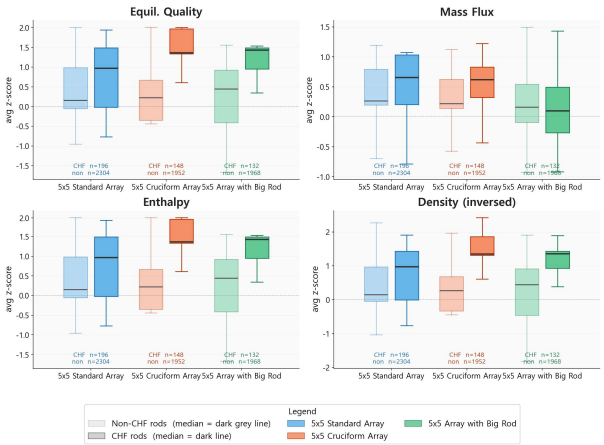

Fig 5. Impact of thermal-hydraulic parameters between CHF rods and non-CHF rods

4. Conclusion

This study assessed the predictive performance of the B&W-2, W-3, and WRB-1 CHF correlations using MATRA for several 5×5 fuel assembly geometries. Among the three models, the W-3 correlation showed the best overall agreement with the experimental data, with mean P/M values closest to unity and relatively low variance. The B&W-2 correlation consistently underpredicted CHF, resulting in conservative thermal margin estimates, while the WRB-1 correlation generally overpredicted CHF.

In the CHF location analysis for assessment of reliable MDNBR evaluation, although B&W-2 and W-3 identified the correct CHF rod, both predicted CHF at multiple rods, indicating conservative but physically less accurate local thermal-hydraulic distributions. WRB-1, in contrast, frequently failed to predict the actual CHF rod. These results confirm that existing CHF correlations have limited capability in predicting not only CHF magnitude but also its occurrence location, primarily because it includes overly strong effects of mixing-vane compared to other correlations based on simple grid.

Overall, the existing correlations do not guarantee robust CHF prediction over a wide range of geometries and operating conditions. This highlights the need for a more universal CHF prediction methodology capable of accurately capturing local thermal-hydraulic behavior and CHF occurrence in various fuel assembly configurations. Therefore, based on the insights obtained in this study, future work will focus on developing a universal machine-learning based CHF prediction model that can robustly account for local thermal-hydraulic behavior and maintain predictive performance across broader geometrical and experimental conditions.

ACKNOWLEDGEMENT

This work was supported by the National Research Foundation of Korea (NRF) grant funded by the Korea government (MSIT) (No. RS-2025-02654004) and Nuclear Safety Research Program through the Regulatory Research Management Agency for SMRs (RMAS) and the Nuclear Safety and Security Commission (NSSC) of the Republic of Korea (No. RS-2025-02309978).

REFERENCES

[1] D. H. Hwang, “Development and Application of Subchannel Analysis Code Technology for Advanced Reactor Systems”, Korea Atomic Energy Research Institute, Daejeon, South Korea, Rep. KAERI/TR-3129/2006, Jan. 2006.
[2] C. F. Fighetti, D. G. Reddy, “Parametric Study of CHF Data, Vol. 3: Critical Heat Flux Data”, Electric Power Research Institute, Palo Alto, CA, USA, Rep. NP-2609, Sep. 1982.
[3] J. S. Gellerstedt et al., "Two-phase flow and heat transfer in rod bundles," in Proc. ASME Winter Annual Meeting, Los Angeles, CA, USA, Nov. 1969, pp. 63–71.
[4] L.S. Tong, “Boiling Crisis and Critical Heat Flux”, U.S. Atomic Energy Commission, Oak Ridge, TN, USA, TID-25887. 1972.
[5] R. C. Anderson, N. P. Wolfhope, “Qualification of the WRB-1 CHF Correlation in the Virginia Power COBRA Code”, Virginia Power, Richmond, VA, USA, Tech. Rep VEP-NE-3, Nov. 1986.